CHINESE OPTICS LETTERS

Vol. 21, No. 4 | April 2023

W-band radio-over-fiber transmission system with delta-sigma modulation and direct detection

Zhou Ju (睢 洲), Jiaxuan Liu (刘家轩), and Jianjun Yu (余建军)*

Key Laboratory for Information Science of Electromagnetic Waves (MoE), Fudan University, Shanghai 200433, China

*Corresponding author: jianjun@fudan.edu.cn

Received November 11, 2022 | Accepted January 6, 2023 | Posted Online March 24, 2023

We experimentally built a W-band photonics-aided millimeter-wave radio-over-fiber transmission system and demonstrated the delivery of up to 8192-ary quadrature amplitude modulation (QAM) signal. Discrete multitone signals are converted into 1-bit data streams through delta-sigma modulation and then modulated onto a 76.2 GHz carrier. An envelope detector is used at the receiver side for direct detection. The results prove that our proposed system can support 2048QAM and 8192QAM transmission while meeting the hard decision forward error correction threshold of 3.8×10^{-3} and the soft decision forward error correction threshold of 4.2×10^{-2}, respectively. We believe this cost-effective scheme is a promising candidate for future high-order QAM millimeter-wave downlink transmission.

Keywords: radio-over-fiber millimeter-wave transmission; W-band; delta-sigma modulation; direct detection; photonics-aided technique.

DOI: 10.3788/COL202321.040602

1. Introduction

Due to the exponential growth of data traffic, millimeter-wave (MMW) communication has become a hot research topic in recent years because of its large available bandwidth. Meanwhile, fiber wireless integration (FWI) technology, which can make full advantage of both the stability of fiber communication and the flexibility of wireless communication, seems to be a promising solution to provide a high-speed and reliable information access in the 5G era[1–6]. On one hand, optical fibers will continue to serve as the main transmission medium for long-distance delivery in the future radio access network (RAN) (e.g., the link to connect central and remote units). On the other hand, wireless networks can be deployed in special areas where it is inconvenient to lay the fibers, or as the extension for the fiber links so that seamless "last-mile" connections for the end-users can be realized[7–10]. Therefore, the research and demonstration of MMW radio-over-fiber (RoF) communication systems would be meaningful for future application.

The feasibility of long-distance high-speed MMW transmission has already been demonstrated, in which different MMW generation methods and multidimensional multiplexing techniques are employed[11–19]. However, there is still some modification we can make on the existing MMW-RoF schemes to improve the cost-effectiveness. At the transmitter side, photonics-aided MMW signal generation technologies can be adopted to overcome the limitation of bandwidth-insufficient electrical devices[20–22]. At the receiver side, we can simply use an envelope detector (ED) to replace the function of a coherent detector, which usually includes expensive high-speed mixers and MMW local oscillators (LOs). An easy-to-implement intensity modulation direct detection (IM/DD) scheme can not only reduce the system cost, but also avoid the frequency-drift issue caused by the linewidth of lasers[23–26]. It is worth noting that high-order modulation formats have long been used to increase system capacity. Unfortunately, considering the saturation effect of envelope detection, multilevel pulse amplitude modulation (PAM) signals or high-order quadrature amplitude modulation (QAM) signals might suffer from severe distortion problems in an IM/DD scheme. Therefore, delta-sigma modulation (DSM), which has drawn increasing attention in recent years, can be introduced to solve this problem. By oversampling and noise shaping, 1-bit DSM can convert signals of any format, no matter how high the modulation order is, into 1-bit data streams, that is, on–off keying (OOK) signals. Besides avoiding the influence of the saturation effect, DSM can also help improve the signal-to-noise ratio (SNR) as well as reduce the system cost and the complexity of the digital signal processing (DSP) algorithms at the receiver side[27–31].

In this paper, a cost-effective W-band IM/DD MMW-RoF system is demonstrated and verified. At the transmitter side, we first convert QAM symbols (up to 8192QAM) into discrete multitone (DMT) format, which are then modulated into OOK signals through DSM and loaded onto a 76.2 GHz frequency carrier. The MMW is generated using the photonics-aided method. After being transmitted over a 1-m wireless link, the MMW is collected and then downconverted by an ED for further

processing. Experimental results show that the 10-Gbaud 2048QAM signal can be transmitted at a bit error rate (BER) lower than 3.8×10^{-3}, while the 10-Gbaud 8192QAM signal can be transmitted at a BER lower than 4.2×10^{-2}, which means post forward error correction (post-FEC) error-free data transmission can be realized. Due to the characteristics of the IM/DD method and the ability to avoid the employment of digital-to-analog converters (DACs) at the base stations, we believe our scheme is advantageously applicable to a low-cost downlink path in a RoF system.

2. Principle of DSM

The Nyquist theorem says that the minimum value of sampling rate f_s should be twice the signal bandwidth BW, i.e., $f_{s,\min} = 2\,\mathrm{BW}$. However, a delta-sigma modulator samples the signal at a rate much higher than this. We define the oversampling ratio (OSR) as $f_s/2\,\mathrm{BW}$. DSM can convert multilevel PAM or DMT signals into OOK format by oversampling and noise shaping. Since oversampling expands the Nyquist zone, different noise transfer functions (NTFs) can be applied to squeeze more quantization noise out of the signal band. The whole process of DSM is equivalent to letting the desired signal and the uniformly distributed quantization noise pass through an all-pass filter and a high-pass filter, respectively[32,33].

Generally speaking, the higher the OSR and the order of NTF are, the better the noise shaping effect will be. In our experiment, the order of NTF is 2, while the OSR is fixed to be 8. Figure 1 depicts the structure of the 1-bit second-order delta-sigma modulator using a cascade of resonators with distributed feedback (CRFB) configuration. The output data stream of DSM, which contains $+1$ and -1, is generated after the comparator. Figure 2 shows the signal transfer function (STF), NTF, and the pole-zero pattern of the delta-sigma modulator we used in the experiment. The x axis representing the normalized frequency is in the logarithmic format. It can be found that the quantization noise will be pushed into the high-frequency region, while the desired signal remains within its original low-frequency band. Therefore, at the receiver side, the original data can be retrieved by simply using a low-pass filter as long as we can recover the OOK signal, which is obviously much easier than recovering high-order PAM or DMT signals directly.

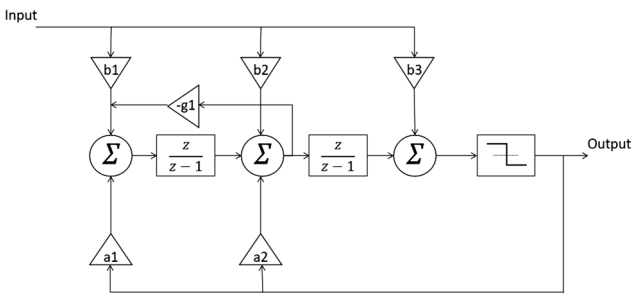

Fig. 1. Structure of the 1-bit second-order delta-sigma modulator with a CRFB configuration.

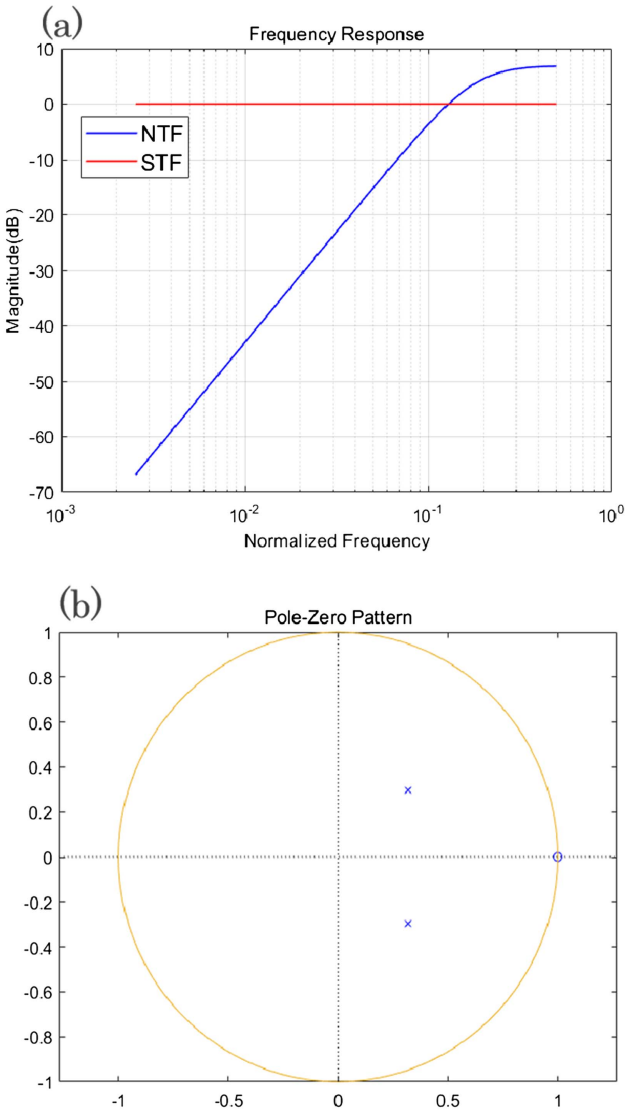

Fig. 2. (a) STF, NTF and (b) the pole-zero pattern of the delta-sigma modulator.

3. Experimental Setup

Figure 3 shows the experimental setup and DSP block diagram of our IM/DD MMW-RoF system with DSM.

We first map binary pseudo-random bits into QAM symbols. They are then converted into a DMT signal with a fast Fourier transform size of 1024 and a cyclic prefix length of 32. The first subcarrier (DC component) is set to 0 while the following 500 (2nd–501st) are used to carry the data. The 502nd to 524th subcarriers are set to 0, and the remaining (525th–1024th subcarriers) are set to be the conjugate symmetry of the 2nd to 501st subcarriers. In order to increase the net data rate, there are no pilots used. After serialization, 2-times upsampling, and baseband shaping through a root-raised cosine (RRC) filter, the DMT signal is oversampled to meet the OSR requirement for DSM. The 1-bit second-order delta-sigma modulator with an OSR of 8 is simulated by MATLAB. The DMT signal is converted into OOK format through DSM, which is then loaded into an

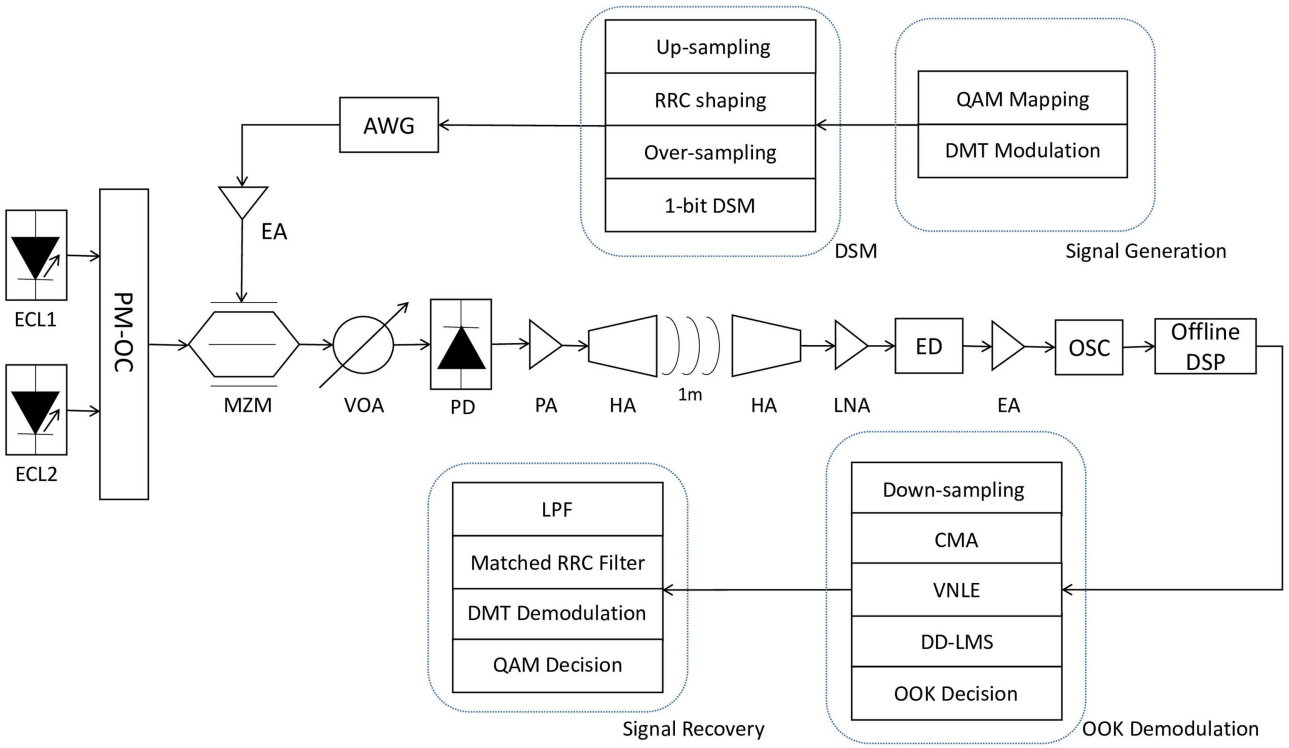

Fig. 3. Experimental setup and DSP block diagram of the proposed IM/DD MMW-RoF system with DSM.

arbitrary waveform generator (AWG) (Tektronix 7122C). The output voltage of the AWG is $0.5V_{pp}$. With the boost of a 30 dB electric amplifier (EA), the data sequence generated by the AWG is used to drive a Mach–Zehnder modulator (MZM) (FTM7938EZ) with 40 GHz bandwidth for electrical-to-optical conversion. The MZM is operating near the quadrature point, and it is ensured that the signal amplitude remains within its linear driving region.

At the transmitter side, two external cavity lasers (ECLs) with linewidth less than 100 kHz produce continuous-wavelength (CW) light waves at 1550 and 1550.61 nm with a frequency spacing of 76.2 GHz. These two laser beams are combined by a polarization-maintaining optical coupler (PM-OC) and then sent into the MZM as the optical carrier. The insertion loss of the MZM is 9 dB. The output signal of the MZM is sent into a photodiode (PD) with a bandwidth of 70 GHz at 6 dB through a variable optical attenuator (VOA). The VOA is used to adjust the input optical power into the PD, which performs square-law detection on the optical signal so that an electrical signal at the frequency of 76.2 GHz can be generated. After being boosted by a power amplifier (PA) with a gain of 21 dB, the W-band MMW signal is sent into free space and then amplified and captured by a pair of horn antennas with 25 dBi gain. The length of the fiber used to generate the signal is 2 m, and the length of the wireless link is 1 m. At the receiver side, the received MMW signal is first amplified by a W-band low-noise amplifier (LNA) and then downconverted to a baseband OOK signal by an ED. The baseband signal is amplified by a 30-dB-gain EA and finally captured by a real-time oscilloscope (OSC) with a bandwidth of 16 GHz. The sampling rate of the OSC is 25 GSa/s.

For the Rx-side offline DSP, the captured signal is processed by downsampling, 51-tap constant modulus algorithm (CMA) equalization, third-order Volterra nonlinear equalization (VNLE), 61-tap direct decision least mean square (DD-LMS) algorithm, and OOK decision. After the OOK signal is recovered, it is sent into a low-pass filter and a matched RRC filter successively for DSM demodulation. Finally, we can acquire the original QAM symbols and binary data through conventional DMT signal-processing techniques.

4. Results and Discussion

Figure 4(a) shows the signal power spectral density after DSM, from which we can find that the SNR of the baseband signal reaches above 30 dB, meaning the noise-shaping performance of the delta-sigma modulator can meet our expectation. The noise of quantization error has been successfully pushed out of the baseband part to the high-frequency region through DSM. Figure 4(b) is the power spectral density of the signal captured by the OSC. Despite the deterioration brought by the fiber and wireless transmission, the SNR of the baseband signal still remains around 20 dB, which grants the feasibility of signal recovery.

For data transmission using DSM, error vector magnitude (EVM) is always used as a performance evaluating indicator. Since our OSR is fixed to be 8, the value of EVM will not fluctuate in a wide range if the parameters are set properly. Therefore, we first measured the EVM between the transmitted and received 1024/2048/4096/8192QAM signals at a baud rate

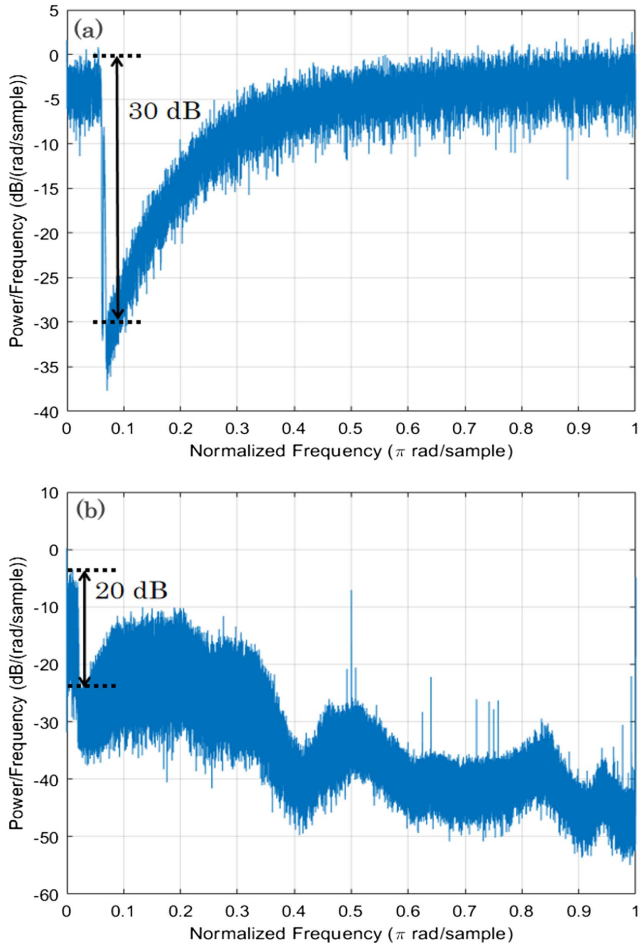

Fig. 4. Power spectral density of the signal (a) after DSM and (b) captured by the OSC.

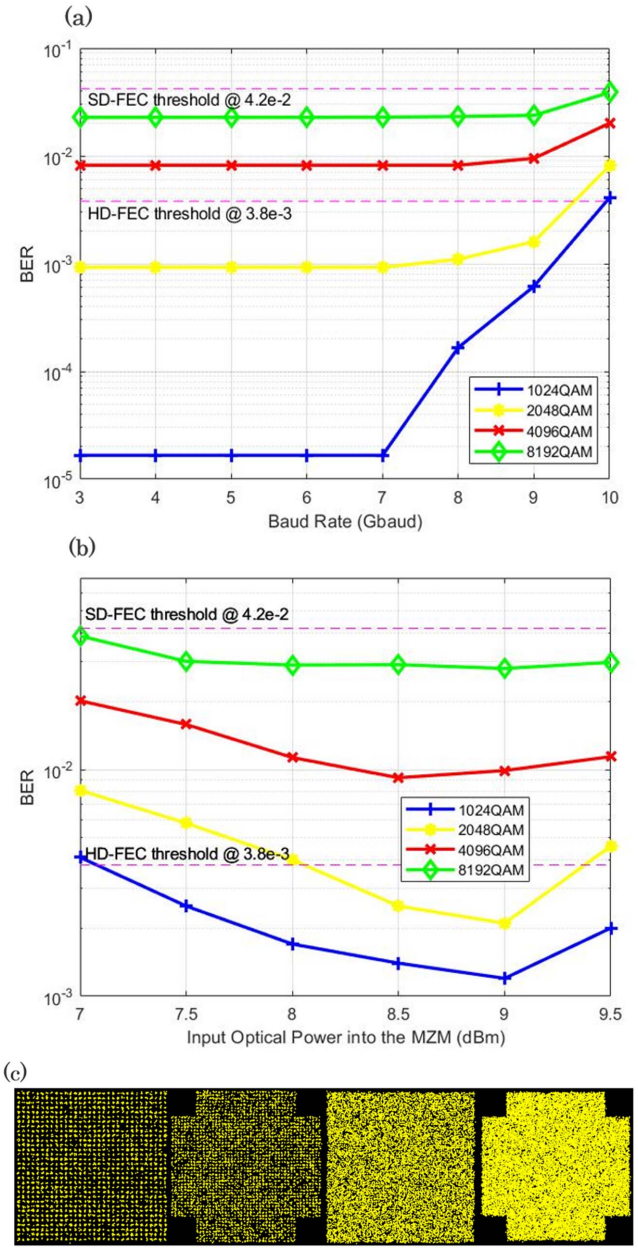

Fig. 5. (a) BER versus baud rate when the input optical power into the MZM is 7 dBm; (b) BER versus input optical power into the MZM when the baud rate is 10 Gbaud; (c) recovered constellation diagrams for different QAM orders.

of 8 Gbaud. When the input optical power into the MZM is 7 dBm, the results are 1.32%, 1.37%, 1.40%, and 1.38%, respectively. Considering the 1.5% EVM threshold corresponding to 4096QAM specified by TS 36.104 V16.9.0[34], we have the anticipation that our proposed system should be able to support at least 4096QAM signal transmission.

After that, we measured the BER performance of 1024/2048/4096/8192QAM signal under different baud rate (3–10 Gbaud) when the input optical power into the MZM is 7 dBm; the result is shown in Fig. 5(a). It can be seen that the performance deteriorates with the increase of baud rate. However, the BER still remains under the soft-decision threshold (4.2×10^{-2} at 25% soft decision FEC), even for the 8192QAM signal at 10 Gbaud. That is to say, after 1-m wireless delivery, post-FEC error-free transmission can be achieved. Furthermore, we can find that for the 10-Gbaud 1024QAM and 2048QAM signals, the BER stands only a little higher than the hard decision threshold (3.8×10^{-3} at 7% hard decision FEC). Therefore, we alter the input optical power to conduct more experiments. Figure 5(b) gives the measured BER versus different input optical power into the MZM (7–9.5 dBm) at a baud rate of 10 Gbaud. With the increase of the input optical power, the performance first improves and then deteriorates. The deterioration is due to the saturation effect of the PD. As shown in Fig. 5(b), when the input optical power reaches 8.5 dBm, the BER of both 1024QAM and 2048QAM signals is below the hard-decision threshold of 3.8×10^{-3}. Post-FEC error-free transmission can thus be achieved at a smaller cost.

Figure 5(c) depicts the corresponding recovered constellation diagrams for 1024/2048/4096/8192QAM signal, respectively. We can calculate the line bit rate we have achieved in the proposed system, that is, 10 × 500 × 13/[1024 × 2 × 8 × (1 + 25%)] = 3.17 Gbit/s for the 10-Gbaud 8192QAM signal with

a redundancy cost of 25%, and $10 \times 500 \times 11/[1024 \times 2 \times 8 \times (1 + 7\%)] = 3.14$ Gbit/s for the 10-Gbaud 2048QAM signal with a redundancy cost of 7%.

5. Conclusion

In this Letter, we have demonstrated a W-band IM/DD MMW-RoF system using DSM, in which QAM signals (up to 8192QAM) are transmitted over optical fiber and a 1-m wireless link. It proves that the BER of the 10-Gbaud 2048QAM signal can meet the HD-FEC threshold of 3.8×10^{-3}, while the BER of the 10-Gbaud 8192QAM signal can meet the SD-FEC threshold of 4.2×10^{-2}. Therefore, post-FEC error-free transmission can be achieved. Considering its excellent cost-effectiveness, we believe that our proposed scheme can be a promising candidate for MMW downlink transmission of high-order QAM signals in the future RAN.

Acknowledgement

This work was partially supported by the National Key R&D Program of China (No. 2018YFB1801703) and the National Natural Science Foundation of China (Nos. 62127802 and 61720106015).

References

1. L. Zhao and J. Yu, "10 Gb/s 16-quadrature amplitude modulation signal delivery over a wireless fiber system by using a directly modulated laser for electrical/optical conversion," Chin. Opt. Lett. **13**, 060601 (2015).
2. J. Xiao, C. Tang, X. Li, J. Yu, X. Huang, C. Yang, and N. Chi, "Polarization multiplexing QPSK signal transmission in optical wireless-over fiber integration system at W-band," Chin. Opt. Lett. **12**, 050603 (2014).
3. M. Wu, J. Zhang, M. Zhu, S. Gao, Z. Wang, X. Liu, B. Hua, Y. Cai, M. Lei, Y. Zou, Q. Li, Y. Wei, W. Tong, and A. Li, "Cost-efficient fiber-wireless-fiber integration system at 28-GHz Ka-band for 5G millimeter-wave coverage scenario," in *19th International Conference on Optical Communications and Networks (ICOCN)* (2021), p. 01.
4. G. -K. Chang and L. Cheng, "Fiber-wireless integration for future mobile communications," in *IEEE Radio and Wireless Symposium (RWS)* (2017), p. 16.
5. X. Li, J. Yu, J. Xiao, and Y. Xu, "Fiber-wireless-fiber link for 128-Gb/s PDM-16QAM signal transmission at W-band," IEEE Photon. Technol. Lett. **26**, 1948 (2014).
6. J. Yu, X. Li, and W. Zhou, "Tutorial: broadband fiber-wireless integration for 5G+ communication," APL Photonics **3**, 111101 (2019).
7. J. Terada, T. Shimada, and A. Otaka, "Optical access network technologies for future radio access networks," in *IEEE Photonics Society Summer Topical Meeting Series (SUM)* (2017), p. 37.
8. Y. Cai, X. Gao, Y. Ling, B. Xu, and K. Qiu, "Power-efficient heterodyne radio over fiber link with laser phase noise robustness," Chin. Opt. Lett. **17**, 110602 (2019).
9. T. Pfeiffer, "Next generation mobile fronthaul and midhaul architectures [Invited]," J. Opt. Commun. Netw. **7**, B38 (2015).
10. C. Lim, Y. Tian, C. Ranaweera, T. A. Nirmalathas, E. Wong, and K. Lee, "Evolution of radio-over-fiber technology," J. Light. Technol. **37**, 1647 (2019).
11. B. Zhu, Y. Wang, W. Li, F. Wang, J. Liu, M. Kong, and J. Yu, "Delivery of 40 Gbit/s W-band signal over 4600 m wireless distance employing advanced digital signal processing," Chin. Opt. Lett. **20**, 103901 (2022).
12. X. Li, J. Yu, L. Zhao, K. Wang, C. Wang, M. Zhao, W. Zhou, and J. Xiao, "1-Tb/s millimeter-wave signal wireless delivery at D-band," J. Light. Technol. **37**, 196 (2019).
13. K. Wang, W. Zhou, L. Zhao, F. Zhao, and J. Yu, "Bi-directional OFDM truncated PS-4096QAM signals transmission in a full-duplex MMW-RoF system at E-band," J. Light. Technol. **39**, 3412 (2021).
14. X. Li, J. Xiao, and J. Yu, "Long-distance wireless mm-wave signal delivery at W-band," J. Light. Technol. **34**, 661 (2016).
15. L. Zhao, K. Wang, W. Zhou, M. Kong, Y. Wang, F. Wang, J. Xiao, and J. Yu, "Demonstration of 73.15 Gbit/s 4096-QAM OFDM D-band wireless transmission employing probabilistic shaping and Volterra nonlinearity compensation," in *European Conference on Optical Communications (ECOC)* (2020), p. 1.
16. M. Kong, W. Zhou, J. Ding, W. Li, and J. Yu, "Simultaneous generation of wired and wireless signals using a DP-MZM in a RoF system," IEEE Photon. Technol. Lett. **32**, 905 (2020).
17. X. Li, J. Yu, J. Zhang, F. Li, and J. Xiao, "Antenna polarization diversity for 146 Gb/s polarization multiplexing QPSK wireless signal delivery at W-band," in *Optical Fiber Communication Conference (OFC)* (2014), paper M3D.7.
18. X. Li, J. Yu, and J. Xiao, "Demonstration of ultra-capacity wireless signal delivery at W-band," J. Light. Technol. **34**, 180 (2016).
19. F. Wang, J. Yu, Y. Wang, W. Li, B. Zhu, J. Ding, K. Wang, C. Liu, C. Wang, M. Kong, L. Zhao, F. Zhao, and W. Zhou, "Delivery of polarization-division-multiplexing wireless millimeter-wave signal over 4.6-km at W-band," J. Light. Technol. **40**, 6339 (2022).
20. Y. Wang, K. Wang, W. Zhou, and J. Yu, "Photonic aided vector millimeter-wave signal generation without digital-to-analog converter," Chin. Opt. Lett. **19**, 011101 (2021).
21. W. Li, M. Li, and N. Zhu, "Photonic generation of background-free millimeter-wave ultra-wideband signals (Invited Paper)," Chin. Opt. Lett. **15**, 010007 (2017).
22. X. Li, J. Yu, and G. -K. Chang, "Photonics-aided millimeter-wave technologies for extreme mobile broadband communications in 5G," J. Light. Technol. **38**, 366 (2020).
23. C. Li, M. Wu, C. Lin, and C. Lin, "W-band OFDM RoF system with simple envelope detector down-conversion," in *Optical Fiber Communications Conference and Exhibition (OFC)* (2015), p. 1.
24. K. Wang, M. Zhao, M. Kong, and J. Yu, "Demonstration of 4 × 100 Gbit/s PAM-4 transmission over 40 km in an IM/DD system based on narrow band DMLs," IEEE Photon. J. **12**, 7201908 (2020).
25. J. Chen, L. Fang, Q. Zhang, J. Zhang, Y. Song, Y. Li, and M. Wang, "Experimental demonstration of 60 Gb/s optical OFDM transmissions at 1550 nm over 100 m OM1 MMF IMDD system with central launching," Chin. Opt. Lett. **15**, 060603 (2017).
26. P. Li, L. Zhu, X. Zhou, W. Pan, H. Zhang, N. Zhong, and L. Yan, "Constant-envelope OFDM for power-efficient and nonlinearity-tolerant heterodyne MMW-RoF system with envelope detection," J. Light. Technol. **40**, 6882 (2022).
27. M. Pessoa, J. S. Tavares, D. Coelho, and H. M. Salgado, "Experimental evaluation of a digitized fiber-wireless system employing sigma delta modulation," Opt. Express **22**, 17508 (2014).
28. J. Wang, Z. Jia, L. A. Campos, and C. Knittle, "Delta-sigma modulation for next generation fronthaul interface," J. Light. Technol. **37**, 2838 (2019).
29. S. Luo, Z. Li, C. Fan, X. Zhu, K. Lv, and Y. Song, "Digital mobile fronthaul based on delta-sigma modulation employing a simple self-coherent receiver," Opt. Express **30**, 30684 (2022).
30. J. Wang, Z. Yu, K. Ying, J. Zhang, F. Lu, M. Xu, L. Cheng, X. Ma, and G. Chang, "Digital mobile fronthaul based on delta-sigma modulation for 32 LTE carrier aggregation and FBMC signals," J. Opt. Commun. Netw. **9**, A233 (2017).
31. F. Olofsson, L. Aabel, M. Karlsson, and C. Fager, "Comparison of transmitter nonlinearity impairments in externally modulated sigma-delta-over fiber vs analog radio-over-fiber links," in *Optical Fiber Communications Conference and Exhibition (OFC)* (2022), p. 1.
32. J. M. de la Rosa, "Sigma-delta modulators: tutorial overview, design guide, and state-of-the-art survey," IEEE Trans. Circuits Syst. I: Regul. Pap. **58**, 1 (2011).
33. K. Bai, D. Zou, Z. Zhang, Z. Li, W. Wang, Q. Sui, Z. Cao, and F. Li, "Digital mobile fronthaul based on performance enhanced multi-stage noise-shaping delta-sigma modulator," J. Light. Technol. **39**, 439 (2021).
34. https://standards.iteh.ai/catalog/standards/etsi/f4be3eb2-7f17-4072-8d0f-71b84378a52f/etsi-ts-136-104-v16-9-0-2021-04